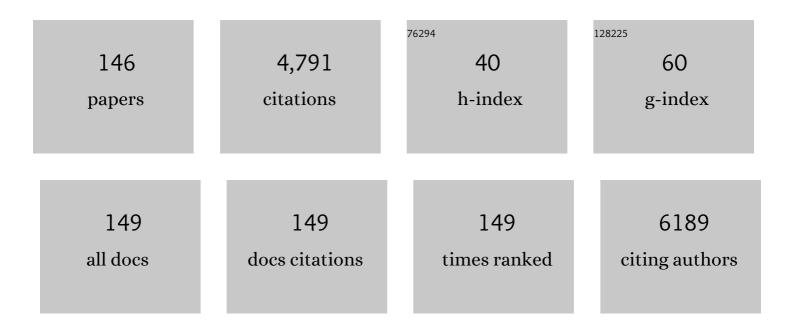
## Luming Peng

List of Publications by Year in descending order

Source: https://exaly.com/author-pdf/8107562/publications.pdf Version: 2024-02-01



#	Article	IF	CITATIONS
1	Ultrahigh rate capability of 1D/2D polyaniline/titanium carbide (MXene) nanohybrid for advanced asymmetric supercapacitors. Nano Research, 2022, 15, 285-295.	5.8	50
2	Identification of CO2 adsorption sites on MgO nanosheets by solid-state nuclear magnetic resonance spectroscopy. Nature Communications, 2022, 13, 707.	5.8	17
3	Nest-type NCMÂâŠ,ÂPt/C with oxygen capture character as advanced electrocatalyst for oxygen reduction reaction. Journal of Energy Chemistry, 2022, 71, 304-312.	7.1	21
4	Subtle modulation on electronic properties of platinum by Cu-Nx containing carbon support for highly efficient electrocatalytic hydrogen evolution. Applied Surface Science, 2022, 591, 153057.	3.1	7
5	Enhancing ionic conductivity in solid electrolyte by relocating diffusion ions to under-coordination sites. Science Advances, 2022, 8, eabj7698.	4.7	37
6	A green route for the preparation of layered double hydroxides from basic magnesium carbonate. Magnetic Resonance Letters, 2022, , .	0.7	3
7	Ternary heterostructural CoO/CN/Ni catalyst for promoted CO2 electroreduction to methanol. Journal of Catalysis, 2021, 393, 83-91.	3.1	20
8	Schiff-base silver nanocomplexes formation on natural biopolymer coated mesoporous silica contributed to the improved curative effect on infectious microbes. Nano Research, 2021, 14, 2735-2748.	5.8	29
9	Surface acidity of tin dioxide nanomaterials revealed with <sup>31</sup> P solid-state NMR spectroscopy and DFT calculations. RSC Advances, 2021, 11, 25004-25009.	1.7	3
10	From helices to superhelices: hierarchical assembly of homochiral van der Waals 1D coordination polymers. Chemical Science, 2021, 12, 12619-12630.	3.7	9
11	TM LDH Meets Birnessite: A 2Dâ€2D Hybrid Catalyst with Longâ€Term Stability for Water Oxidation at Industrial Operating Conditions. Angewandte Chemie - International Edition, 2021, 60, 9699-9705.	7.2	57
12	Ultrasonic assisted growth of SnO2@carbon hollow nanosphere composites as conductive agent free anode materials for lithium-ion batteries. Ionics, 2021, 27, 1949-1955.	1.2	1
13	TM LDH Meets Birnessite: A 2Dâ€2D Hybrid Catalyst with Longâ€Term Stability for Water Oxidation at Industrial Operating Conditions. Angewandte Chemie, 2021, 133, 9785-9791.	1.6	3
14	7Li NMR investigations of Li/MgO catalysts for oxidative coupling of methane. Molecular Catalysis, 2021, 513, 111802.	1.0	1
15	Layer structural MoO2/carbon hybrid composites as anode materials for lithium-ion batteries. Ionics, 2021, 27, 4713-4720.	1.2	1
16	Enzyme-like mechanism of selective toluene oxidation to benzaldehyde over organophosphoric acid-bonded nano-oxides. Chinese Journal of Catalysis, 2021, 42, 1509-1518.	6.9	12
17	Electronic Structure of Anode Material Li <sub>2</sub> TiSiO <sub>5</sub> and Its Structural Evolution during Lithiation. Journal of Physical Chemistry C, 2021, 125, 3733-3744.	1.5	3
18	Enhanced Fluoride Uptake by Layered Double Hydroxides under Alkaline Conditions: Solid-State NMR Evidence of the Role of Surface >MgOH Sites. Environmental Science & Technology, 2021, 55, 15082-15089.	4.6	22

#	Article	IF	CITATIONS
19	Exclusively catalytic oxidation of toluene to benzaldehyde in an O/W emulsion stabilized by hexadecylphosphate acid terminated mixed-oxide nanoparticles. Chinese Journal of Catalysis, 2020, 41, 341-349.	6.9	24
20	Morphologyâ€Reserved Synthesis of Discrete Nanosheets of CuO@SAPOâ€34 and Pore Mouth Catalysis for Oneâ€Pot Oxidation of Cyclohexane. Angewandte Chemie, 2020, 132, 2628-2633.	1.6	12
21	Morphologyâ€Reserved Synthesis of Discrete Nanosheets of CuO@SAPOâ€34 and Pore Mouth Catalysis for Oneâ€Pot Oxidation of Cyclohexane. Angewandte Chemie - International Edition, 2020, 59, 2606-2611.	7.2	36
22	Adjacent acid sites cooperatively catalyze fructose to 5-hydroxymethylfurfural in a new, facile pathway. Journal of Energy Chemistry, 2020, 47, 112-117.	7.1	20
23	γ-Al2O3 sheet-stabilized isolate Co2+ for catalytic propane dehydrogenation. Journal of Catalysis, 2020, 381, 482-492.	3.1	98
24	Dialing in Catalytic Sites on Metal Organic Framework Nodes: MIL-53(Al) and MIL-68(Al) Probed with Methanol Dehydration Catalysis. ACS Applied Materials & Interfaces, 2020, 12, 53537-53546.	4.0	34
25	Iron oxide encapsulated in nitrogen-rich carbon enabling high-performance lithium-ion capacitor. Science China Materials, 2020, 63, 2289-2302.	3.5	13
26	CO2 Hydrogenation to Ethanol over Cu@Na-Beta. CheM, 2020, 6, 2673-2689.	5.8	130
27	Crystal-Facet Modulated CrO <sub><i>x</i></sub> /γ-Al <sub>2</sub> O <sub>3</sub> : Quasi-Liquid Surface Modification by Bonded Polydimethylsiloxane for Catalytic Oxidation of Propene. Langmuir, 2020, 36, 10404-10411.	1.6	2
28	Atomically dispersed Lewis acid sites boost 2-electron oxygen reduction activity of carbon-based catalysts. Nature Communications, 2020, 11, 5478.	5.8	114
29	Interactions of Oxide Surfaces with Water Revealed with Solid-State NMR Spectroscopy. Journal of the American Chemical Society, 2020, 142, 11173-11182.	6.6	24
30	TiO2 modified α-Fe2O3 pompon-like hollow sphere as the anode material for lithium-ion batteries with mixed lithiation mechanisms. Ionics, 2020, 26, 2781-2790.	1.2	3
31	Frontispiece: Morphologyâ€Reserved Synthesis of Discrete Nanosheets of CuO@SAPOâ€34 and Pore Mouth Catalysis for Oneâ€Pot Oxidation of Cyclohexane. Angewandte Chemie - International Edition, 2020, 59, .	7.2	0
32	Frontispiz: Morphologyâ€Reserved Synthesis of Discrete Nanosheets of CuO@SAPOâ€34 and Pore Mouth Catalysis for Oneâ€Pot Oxidation of Cyclohexane. Angewandte Chemie, 2020, 132, .	1.6	0
33	Probing Interactions of γâ€Alumina with Water via Multinuclear Solidâ€6tate NMR Spectroscopy. ChemCatChem, 2020, 12, 1569-1574.	1.8	17
34	<sup>17</sup> O Solid-State NMR Studies of Ta <sub>2</sub> O <sub>5</sub> Nanorods. ACS Omega, 2020, 5, 8355-8361.	1.6	7
35	Modulating Lattice Oxygen in Dual-Functional Mo–V–O Mixed Oxides for Chemical Looping Oxidative Dehydrogenation. Journal of the American Chemical Society, 2019, 141, 18653-18657.	6.6	133
36	Hydrophobic Functionalization of ZnO Nanosheets by In Situ Centerâ€Substituted Synthesis for Selective Photocatalysis under Visible Irradiation. Particle and Particle Systems Characterization, 2019, 36, 1800403.	1.2	10

#	Article	IF	CITATIONS
37	Iron oxide encapsulated in nitrogen-doped carbon as high energy anode material for asymmetric supercapacitors. Journal of Power Sources, 2019, 438, 227047.	4.0	25
38	170 Solid-State NMR Studies of ZrO2 Nanoparticles. Journal of Physical Chemistry C, 2019, 123, 4158-4167.	1.5	17
39	Ternary Heterostructural Pt/CNx/Ni as a Supercatalyst for Oxygen Reduction. IScience, 2019, 11, 388-397.	1.9	36
40	Antimony-doped tin oxide nanoparticles as peroxidase mimics for paper-based colorimetric detection of glucose using smartphone read-out. Mikrochimica Acta, 2019, 186, 403.	2.5	34
41	Investigating the Structure of an Active Material–Carbon Interface in the Monoclinic Li <sub>3</sub> V <sub>2</sub> (PO <sub>4</sub> ) <sub>3</sub> /C Composite Cathode. ACS Applied Energy Materials, 2019, 2, 3692-3702.	2.5	9
42	LiNi0.8Co0.15Al0.05O2 cathodes exhibiting improved capacity retention and thermal stability due to a lithium iron phosphate coating. Electrochimica Acta, 2019, 312, 179-187.	2.6	50
43	Promoting defective-Li <sub>2</sub> O <sub>2</sub> formation <i>via</i> Na doping for Li–O <sub>2</sub> batteries with low charge overpotentials. Journal of Materials Chemistry A, 2019, 7, 10389-10396.	5.2	17
44	Polar surface structure of oxide nanocrystals revealed with solid-state NMR spectroscopy. Nature Communications, 2019, 10, 5420.	5.8	41
45	Real-time cell analysis of the cytotoxicity of a pH-responsive drug-delivery matrix based on mesoporous silica materials functionalized with ferrocenecarboxylic acid. Analytica Chimica Acta, 2019, 1051, 138-146.	2.6	14
46	Defect Chemistry in Discharge Products of Li–O <sub>2</sub> Batteries. Small Methods, 2019, 3, 1800358.	4.6	34
47	Recent progress in investigations of surface structure and properties of solid oxide materials with nuclear magnetic resonance spectroscopy. Chinese Chemical Letters, 2018, 29, 747-751.	4.8	18
48	A high-performance asymmetric supercapacitor based on vanadyl phosphate/carbon nanocomposites and polypyrrole-derived carbon nanowires. Nanoscale, 2018, 10, 3709-3719.	2.8	36
49	The effect of electrostatic field on the catalytic properties of platinum clusters confined in zeolite for hydrogenation. Catalysis Science and Technology, 2018, 8, 6384-6395.	2.1	18
50	Intercalation of alkylamines in layered MoO <sub>3</sub> and <i>in situ</i> carbonization for a high-performance asymmetric supercapacitor. Sustainable Energy and Fuels, 2018, 2, 2788-2798.	2.5	21
51	Reduction-oxidation pretreatment enhanced catalytic performance of Co3O4/Al2O3 over CO oxidation. Applied Surface Science, 2018, 453, 330-335.	3.1	24
52	Probing local structure of paramagnetic Ni-Al layered double hydroxides with solid-state 2H NMR spectroscopy. Chemical Physics Letters, 2018, 706, 47-52.	1.2	9
53	Crown ether induced assembly to γ-Al2O3 nanosheets with rich pentacoordinate Al3+ sites and high ethanol dehydration activity. Applied Surface Science, 2018, 457, 626-632.	3.1	22
54	Direct Conversion of Syngas into Methyl Acetate, Ethanol, and Ethylene by Relay Catalysis via the Intermediate Dimethyl Ether. Angewandte Chemie - International Edition, 2018, 57, 12012-12016.	7.2	142

#	Article	IF	CITATIONS
55	Carbon nitride with encapsulated nickel for semi-hydrogenation of acetylene: pyridinic nitrogen is responsible for hydrogen dissociative adsorption. Science China Chemistry, 2018, 61, 1014-1019.	4.2	7
56	Crystal-Facet Effect of γ-Al <sub>2</sub> O <sub>3</sub> on Supporting CrO <sub><i>x</i></sub> for Catalytic Semihydrogenation of Acetylene. ACS Catalysis, 2018, 8, 6419-6425.	5.5	38
57	Dual-Responsive Bola-Type Supra-Amphiphile Constructed from Water-Soluble Pillar[5]arene and Naphthalimide-Containing Amphiphile for Intracellular Drug Delivery. ACS Applied Materials & Interfaces, 2017, 9, 4843-4850.	4.0	75
58	Surface-selective direct <sup>17</sup> O DNP NMR of CeO <sub>2</sub> nanoparticles. Chemical Communications, 2017, 53, 2142-2145.	2.2	62
59	Platinum nanoparticles encapsulated in HZSM-5 crystals as an efficient catalyst for green production of p-aminophenol. Catalysis Communications, 2017, 97, 98-101.	1.6	21
60	Nanotubular Gamma Alumina with High-Energy External Surfaces: Synthesis and High Performance for Catalysis. ACS Catalysis, 2017, 7, 4083-4092.	5.5	41
61	Cooperativity of adjacent BrÃ,nsted acid sites in MFI zeolite channel leads to enhanced polarization and cracking of alkanes. Journal of Catalysis, 2017, 349, 163-174.	3.1	85
62	Mixed Molybdenum Oxides with Superior Performances as an Advanced Anode Material for Lithium-Ion Batteries. Scientific Reports, 2017, 7, 44697.	1.6	52
63	Topochemical polymerisation of assembled diacetylene macrocycle bearing dibenzylphosphine oxide in solid state. Supramolecular Chemistry, 2017, 29, 94-101.	1.5	5
64	Distinguishing faceted oxide nanocrystals with 17O solid-state NMR spectroscopy. Nature Communications, 2017, 8, 581.	5.8	48
65	Surface titanium oxide loaded on a special alumina as high-performance catalyst for reduction of cinnamaldehyde by isopropanol. Chinese Journal of Catalysis, 2017, 38, 1330-1337.	6.9	2
66	Templateâ€Free Synthesis of Highâ€Content Vanadiumâ€Doped ZSMâ€5 with Enhanced Catalytic Performance. ChemistrySelect, 2017, 2, 11513-11520.	0.7	5
67	3D charged grid induces a high performance catalyst: ruthenium clusters enclosed in X-zeolite for hydrogenation of phenol to cyclohexanone. Catalysis Science and Technology, 2017, 7, 5953-5963.	2.1	32
68	GSH-Responsive supramolecular nanoparticles constructed by β- <scp>d</scp> -galactose-modified pillar[5]arene and camptothecin prodrug for targeted anticancer drug delivery. Chemical Communications, 2017, 53, 8596-8599.	2.2	81
69	Simple Synthesis of TiO2/MnOx Composite with Enhanced Performances as Anode Materials for Li-Ion Battery. Electrochimica Acta, 2016, 211, 832-841.	2.6	19
70	Ni-Silicides nanoparticles as substitute for noble metals for hydrogenation of nitrobenzene to p-Aminophenol in sulfuric acid. Applied Catalysis A: General, 2016, 520, 151-156.	2.2	23
71	An efficient hydrogenation catalyst in sulfuric acid for the conversion of nitrobenzene to p-aminophenol: N-doped carbon with encapsulated molybdenum carbide. Chemical Communications, 2016, 52, 10672-10675.	2.2	24
72	Study of Microstructure Change of Carbon Nanofibers as Binder-Free Anode for High-Performance Lithium-Ion Batteries. ACS Applied Materials & Interfaces, 2016, 8, 33091-33101.	4.0	43

#	Article	IF	CITATIONS
73	CeO <sub>2</sub> nanorods anchored on mesoporous carbon as an efficient catalyst for imine synthesis. Chemical Communications, 2016, 52, 13495-13498.	2.2	49
74	Ultrathin anatase nanosheets with high energy facets exposed and related photocatalytic performances. RSC Advances, 2016, 6, 62675-62679.	1.7	2
75	Solvent-free synthesis of crystalline mesoporous γ-Fe <sub>2</sub> O <sub>3</sub> as an anode material in lithium-ion batteries. RSC Advances, 2016, 6, 57009-57012.	1.7	10
76	Controllable Construction of Biocompatible Supramolecular Micelles and Vesicles by Water-Soluble Phosphate Pillar[5,6]arenes for Selective Anti-Cancer Drug Delivery. Chemistry of Materials, 2016, 28, 3778-3788.	3.2	119
77	Identification of different tin species in SnO2 nanosheets with 119Sn solid-state NMR spectroscopy. Chemical Physics Letters, 2016, 643, 126-130.	1.2	15
78	Catalytic hydroxylation enables phenol to efficient assembly of ordered mesoporous carbon under highly acidic conditions. Microporous and Mesoporous Materials, 2016, 223, 114-120.	2.2	18
79	High selectivity top-chloroaniline in the hydrogenation ofp-chloronitrobenzene on Ni modified carbon nitride catalyst. Chinese Journal of Catalysis, 2015, 36, 2030-2035.	6.9	14
80	Oneâ€Pot Synthesis of Zeolitic Strong Solid Bases: A Family of Alkalineâ€Earth Metalâ€Containing Silicaliteâ€1. Chemistry - A European Journal, 2015, 21, 15412-15420.	1.7	23
81	Thickness-dependent SERS activities of gold nanosheets controllably synthesized via photochemical reduction in lamellar liquid crystals. Chemical Communications, 2015, 51, 5116-5119.	2.2	28
82	Dehydration and Dehydroxylation of Layered Double Hydroxides: New Insights from Solid-State NMR and FT-IR Studies of Deuterated Samples. Journal of Physical Chemistry C, 2015, 119, 12325-12334.	1.5	36
83	Identification of different oxygen species in oxide nanostructures with <sup>17</sup> O solid-state NMR spectroscopy. Science Advances, 2015, 1, e1400133.	4.7	72
84	Organic-free synthesis of ultrathin gold nanowires as effective SERS substrates. Chemical Communications, 2015, 51, 11841-11843.	2.2	14
85	Combined desilication and phosphorus modification for high-silica ZSM-5 zeolite with related study of hydrocarbon cracking performance. Applied Catalysis A: General, 2015, 503, 147-155.	2.2	60
86	Identification of intrinsic hydrogen impurities in ZnO with 1H solid-state nuclear magnetic resonance spectroscopy. Chemical Physics Letters, 2015, 627, 7-12.	1.2	15
87	Platinum Nanoparticles Encapsulated in MFI Zeolite Crystals by a Two-Step Dry Gel Conversion Method as a Highly Selective Hydrogenation Catalyst. ACS Catalysis, 2015, 5, 6893-6901.	5.5	136
88	17O solid-state NMR studies of oxygen-containing catalysts. Chinese Journal of Catalysis, 2015, 36, 1494-1504.	6.9	20
89	A sintering-resistant Pd/SiO <sub>2</sub> catalyst by reverse-loading nano iron oxide for aerobic oxidation of benzyl alcohol. RSC Advances, 2015, 5, 4766-4769.	1.7	16
90	Investigating Local Structure in Layered Double Hydroxides with <sup>17</sup> 0 NMR Spectroscopy. Advanced Functional Materials, 2014, 24, 1696-1702.	7.8	32

#	Article	IF	CITATIONS
91	Supramolecular Materials: Investigating Local Structure in Layered Double Hydroxides with170 NMR Spectroscopy (Adv. Funct. Mater. 12/2014). Advanced Functional Materials, 2014, 24, 1695-1695.	7.8	0
92	Partially nitrided molybdenum trioxide with promoted performance as an anode material for lithium-ion batteries. Journal of Materials Chemistry A, 2014, 2, 699-704.	5.2	104
93	Organoamine-assisted biomimetic synthesis of faceted hexagonal hydroxyapatite nanotubes with prominent stimulation activity for osteoblast proliferation. Journal of Materials Chemistry B, 2014, 2, 1760-1763.	2.9	41
94	Probing Local Structure of Layered Double Hydroxides with <sup>1</sup> H Solid-State NMR Spectroscopy on Deuterated Samples. Journal of Physical Chemistry Letters, 2014, 5, 363-369.	2.1	16
95	Hexadecylphosphate-Functionalized Iron Oxide Nanoparticles: Mild Oxidation of Benzyl C–H Bonds Exclusive to Carbonyls by Molecular Oxygen. ACS Catalysis, 2014, 4, 2746-2752.	5.5	20
96	Remarkable acceleration of the fructose dehydration over the adjacent BrÃ,nsted acid sites contained in an MFI-type zeolite channel. Journal of Catalysis, 2014, 319, 150-154.	3.1	18
97	Efficient self-metathesis of 1-butene on molybdenum oxide supported on silica modified one-dimensional γ-Al 2 O 3. Journal of Molecular Catalysis A, 2014, 394, 1-9.	4.8	17
98	MoO <sub>2</sub> @carbon hollow microspheres with tunable interiors and improved lithium-ion battery anode properties. Physical Chemistry Chemical Physics, 2014, 16, 20570-20577.	1.3	41
99	Acid-Resistant Catalysis without Use of Noble Metals: Carbon Nitride with Underlying Nickel. ACS Catalysis, 2014, 4, 2536-2543.	5.5	135
100	Super high selectivity of acrolein in oxidation of propene on molybdenum promoted hierarchical assembly of bismuth tungstate nanoflakes. Applied Catalysis A: General, 2014, 482, 179-188.	2.2	12
101	Highly active gold catalysts loaded on NiAl-oxide derived from layered double hydroxide for aerobic alcohol oxidation. Applied Catalysis A: General, 2014, 482, 294-299.	2.2	16
102	Heteropolyanion-based ionic liquid-functionalized mesoporous copolymer catalyst for Friedel–Crafts benzylation of arenes with benzyl alcohol. Chemical Engineering Journal, 2014, 254, 54-62.	6.6	61
103	Half-encapsulated Au nanoparticles by nano iron oxide: promoted performance of the aerobic oxidation of 1-phenylethanol. Nanoscale, 2013, 5, 9546.	2.8	15
104	Mesostructural Bi-Mo-O catalyst: correct structure leading to high performance. Scientific Reports, 2013, 3, 2881.	1.6	15
105	High performance mesoporous zirconium phosphate for dehydration of xylose to furfural in aqueous-phase. RSC Advances, 2013, 3, 23228.	1.7	42
106	Synergism between the Lewis and Brönsted acid sites on HZSM-5 zeolites in the conversion of methylcyclohexane. Chinese Journal of Catalysis, 2013, 34, 2153-2159.	6.9	22
107	Sandwich-like LiFePO4/graphene hybrid nanosheets: in situ catalytic graphitization and their high-rate performance for lithium ion batteries. Journal of Materials Chemistry A, 2013, 1, 11534.	5.2	81
108	Designed Synthesis of Functionalized Twoâ€Dimensional Metal–Organic Frameworks with Preferential CO <sub>2</sub> Capture. ChemPlusChem, 2013, 78, 86-91.	1.3	48

#	Article	IF	CITATIONS
109	Optimizing activity of tungsten oxides for 1-butene metathesis by depositing silica on γ-alumina support. Chemical Engineering Research and Design, 2013, 91, 573-580.	2.7	46
110	Selective oxidation of toluene using surface-modified vanadium oxide nanobelts. Chinese Journal of Catalysis, 2013, 34, 1297-1302.	6.9	5
111	Solid-State MAS NMR Studies of BrÃ,nsted Acid Sites in Zeolite H-Mordenite. Journal of the American Chemical Society, 2012, 134, 9708-9720.	6.6	85
112	The effects of carbonaceous species in HZSM-5 on methanol-to-olefin process. Applied Catalysis A: General, 2012, 421-422, 108-113.	2.2	15
113	Comparison of preparation and formation mechanism of LuAG nanopowders using two different methods. Micro and Nano Letters, 2012, 7, 529.	0.6	7
114	Inorganic nanotubes formation through the synergic evolution of dynamic templates and metallophosphates: from vesicles to nanotubes. Chemical Communications, 2011, 47, 10061.	2.2	12
115	Nanocrystals of CeVO <sub>4</sub> Doped by Metallic Heteroions. Inorganic Chemistry, 2011, 50, 6189-6194.	1.9	28
116	Iron oxide and alumina nanocomposites applied to Fischer–Tropsch synthesis. Chemical Communications, 2011, 47, 4019.	2.2	44
117	Measuring BrÃ,nsted Acid Site Oâ^'H Distances in Zeolites HY and HZSM-5 with Low-Temperature <sup>17</sup> Oâr' <sup>1</sup> H Double Resonance MAS NMR Spectroscopy. Journal of Physical Chemistry C, 2011, 115, 2030-2037.	1.5	24
118	One-pot synthesis of boron-doped mesoporous carbon with boric acid as a multifunction reagent. Microporous and Mesoporous Materials, 2011, 142, 609-613.	2.2	69
119	Catalytic Ammonia Synthesis over Mo Nitride/ZSMâ€5. ChemCatChem, 2010, 2, 167-174.	1.8	18
120	1-Butene cracking to propene over P/HZSM-5: Effect of lanthanum. Journal of Molecular Catalysis A, 2010, 327, 12-19.	4.8	49
121	Effects of e-beam curing on glass structureand mechanical properties of nanoporous organosilicate thin films. International Journal of Materials Research, 2010, 101, 228-235.	0.1	3
122	Exclusively selective oxidation of toluene to benzaldehyde on ceria nanocubes by molecular oxygen. Chemical Communications, 2010, 46, 5909.	2.2	106
123	Solvothermal synthesis of lutetium aluminum garnet nanopowders: Determination of the optimum synthesis conditions. Journal of Alloys and Compounds, 2010, 491, 599-604.	2.8	10
124	Noncrystalline NiPB nanotubes for hydrogenation of p-chloronitrobenzene. Chemical Communications, 2010, 46, 2268.	2.2	31
125	Silica Nanotubes and Their Assembly Assisted by Boric Acid to Hierachical Mesostructures. Langmuir, 2010, 26, 4572-4575.	1.6	39
126	Ferric oxide and ZnFe2O4 nanotubes derived from nano ZnO/FeOx core/shell structures. Materials Letters, 2009, 63, 2233-2235.	1.3	8

#	Article	IF	CITATIONS
127	Low Temperature <sup>1</sup> H MAS NMR Spectroscopy Studies of Proton Motion in Zeolite HZSM-5. Journal of Physical Chemistry C, 2009, 113, 8211-8219.	1.5	43
128	The hydrophilic/hydrophobic effect of porous solid acid catalysts on mixed liquid phase reaction of esterification. Catalysis Communications, 2009, 10, 1734-1737.	1.6	31
129	Synthesis of VO <i>x</i> Nanotubes by Cooperation of Tetramethylammonium Hydroxide and Tetradecylamine in Short Duration. Chemistry Letters, 2009, 38, 928-929.	0.7	3
130	170 MQMAS NMR studies of zeolite HY. Microporous and Mesoporous Materials, 2008, 109, 156-162.	2.2	28
131	Diphosphine probe molecules and solid-state NMR investigations of proximity between acidic sites in zeolite HY. Microporous and Mesoporous Materials, 2008, 116, 277-283.	2.2	24
132	Variable-Temperature <sup>17</sup> 0 NMR Study of Oxygen Motion in the Anionic Conductor Bi <sub>26</sub> Mo <sub>10</sub> O <sub>69</sub> . Chemistry of Materials, 2008, 20, 3638-3648.	3.2	47
133	High resolution 170 MAS and triple-quantum MAS NMR studies of gallosilicate glasses. Journal of Non-Crystalline Solids, 2008, 354, 3120-3128.	1.5	13
134	Effects of UV cure on glass structure and fracture properties of nanoporous carbon-doped oxide thin films. Journal of Applied Physics, 2008, 104, 043513.	1.1	32
135	Probing brÃ,nsted acid sites in zeolite HY with low temperature 170 MAS NMR spectroscopy. Studies in Surface Science and Catalysis, 2007, 170, 783-789.	1.5	3
136	Germanosilicate and alkali germanosilicate glass structure: New insights from high-resolution oxygen-17 NMR. Journal of Non-Crystalline Solids, 2007, 353, 2910-2918.	1.5	29
137	Sodium germanate glasses and crystals: NMR constraints on variation in structure with composition. Journal of Non-Crystalline Solids, 2007, 353, 4732-4742.	1.5	29
138	170 Magic Angle Spinning NMR Studies of BrÃ,nsted Acid Sites in Zeolites HY and HZSM-5. Journal of the American Chemical Society, 2007, 129, 335-346.	6.6	90
139	17O NMR studies of local structure and phase evolution for materials in the Y2Ti2O7–ZrTiO4 binary system. Journal of Solid State Chemistry, 2007, 180, 2175-2185.	1.4	7
140	Synthesis and Structure Determination of a New Organically Templated Scandium Fluorophosphate Framework and Its Indium Analogue ChemInform, 2005, 36, no.	0.1	0
141	Detection of BrÃ,nsted acid sites in zeolite HY with high-field 17O-MAS-NMR techniques. Nature Materials, 2005, 4, 216-219.	13.3	110
142	Synthesis and Structure Determination of a New Organically Templated Scandium Fluorophosphate Framework and Its Indium Analogue. Chemistry of Materials, 2004, 16, 5350-5356.	3.2	32
143	Measuring BrÃ,nsted Acid Densites in Zeolite HY with Diphosphine Molecules and Solid State NMR Spectroscopy. Journal of the American Chemical Society, 2004, 126, 12254-12255.	6.6	50
144	Hydrothermal Synthesis and Structural Characterization of Four Scandium Phosphate Frameworks ChemInform, 2003, 34, no.	0.1	0

#	Article	IF	CITATIONS
145	Hydrothermal Synthesis and Structural Characterization of Four Scandium Phosphate Frameworks. Chemistry of Materials, 2003, 15, 3818-3825.	3.2	20
146	Sandwich-Like Holey Graphene/PANI/Graphene Nanohybrid for Ultrahigh-Rate Supercapacitor. ACS Applied Energy Materials, 0, , .	2.5	14